

On the nature of XTE J0421+560/CI Cam

T. Belloni^{1,2}, S. Dieters³, M.E. van den Ancker¹, R.P. Fender¹, D.W. Fox⁴, B.A. Harmon⁵, M. van der Klis¹, J.M. Kommers⁴, W.H.G. Lewin⁴, J. Van Paradijs^{1,6}

ABSTRACT

We present the results of the analysis of RXTE, BATSE and optical/infrared data of the 1998 outburst of the X-ray transient system XTE J0421+560 (CI Cam). The X-ray outburst shows a very fast decay (initial e-folding time ~ 0.5 days, slowing down to ~ 2.3 days). The X-ray spectrum in the 2-25 keV band is complex, softening considerably during decay and with strongly variable intrinsic absorption. A strong iron emission line is observed. No fast time variability is detected ($< 0.5\%$ rms in the 1-4096 Hz band at the outburst peak). The analysis of the optical/IR data suggests that the secondary is a B[e] star surrounded by cool dust and places the system at a distance of $\gtrsim 2$ kpc. At this distance the peak 2-25 keV luminosity is $\sim 4 \times 10^{37}$ erg/s. We compare the properties of this peculiar system with those of the Be/NS LMC transient A 0538-66 and suggest that CI Cam is of similar nature. The presence of strong radio emission during outburst indicates that the compact object is likely to be a black hole or a weakly magnetized neutron star.

Subject headings: accretion, accretion disks — binaries: close — X-rays: stars — stars: individual XTE J0421+560/CI Cam

1. INTRODUCTION

On 1998 March 31st, a bright X-ray transient was detected with the All-Sky Monitor (ASM: Levine et al. 1996) on board the Rossi X-ray Timing Explorer (RXTE) (Smith et al. 1998).

¹Astronomical Institute “Anton Pannekoek”, University of Amsterdam and Center for High-Energy Astrophysics, Kruislaan 403, NL-1098 SJ Amsterdam, the Netherlands

²Present address: Osservatorio Astronomico di Brera, Via E. Bianchi 46, I-23807 Merate (LC), Italy

³Center for Space Plasma and Aeronomic Research, University of Alabama in Huntsville, Huntsville, AL 35899, USA

⁴Massachusetts Institute of Technology, Center for Space Research, Room 37-627, Cambridge, MA 02139, USA

⁵NASA Marshall Space Flight Center, Huntsville, AL 35812, USA

⁶Physics Department, University of Alabama in Huntsville, Huntsville, AL 35899, USA

The source brightened quickly, reaching a maximum brightness of ~ 2 Crab a few hours after the discovery, then decaying exponentially with a very short e-folding time (0.6 days, Revnivtsev, Emelyanov & Borozdin 1998). It was also detected with BeppoSAX (Orlandini et al. 1998) and (above 20 keV) with BATSE (Paciesas & Fishman 1998, Harmon, Fishman & Paciasas 1998). ASCA observations of XTE J0421+056 were made three days into the outburst (Ueda et al. 1998). During the ASCA observations the source was fading with an e-folding time of ~ 30 hours and its spectrum was softening. The spectrum above 1 keV was fitted with a two-temperature (1.1 and 5.7 keV) optically thin thermal model and an additional emission feature at 6.4 keV. Interestingly, below 1 keV an additional component was detected, which showed two flares during the observation. Two BeppoSAX observations of the transient confirmed the presence of a very soft variable component in the X-ray spectrum (Frontera et al. 1998, Orr et al. 1998). From the ASCA and the BeppoSAX data, it is evident that the X-ray spectrum between 1 and 10 keV is essentially thermal, with the additional presence of a number of emission lines (Ueda et al. 1998, Orr et al. 1998).

A transient radio counterpart of XTE J0421+560 was detected by Hjellming & Mioduszewski (1998 a,b). The radio position coincides with that of the variable star CI Cam (= MWC 84) which had been classified as a symbiotic star (Bergner et al. 1995). This object, whose visual magnitude is usually $V \sim 11.6$ (Bergner et al. 1995) had brightened by $\gtrsim 3.5$ magnitudes in the R band (Robinson et al. 1998) and by >2 magnitudes in B and V (Garcia et al. 1998, Hynes et al. 1998). The optical outburst was also apparently very rapid. A comparison of the available outburst photometry with historical photometry, shows that CI Cam returned to within one magnitude from quiescence on April 6th, i.e. the outburst lasted ≈ 6 days. The optical spectrum showed He II lines in addition to the complex emission features observed in quiescence, but no indication of binarity was found (Wagner & Starrfield 1998).

In the radio, double S-shaped jets, moving at an apparent velocity of $0.15c$ (for a distance of 1 kpc), have been reported (Hjellming & Mioduszewski 1998b).

Overall, almost all the observed properties of XTE J0421+560/CI Cam are rather peculiar and do not allow a straightforward classification of the system beyond the assessment of the presence of a compact object, given the large X-ray luminosity.

Here we present results of our analysis of the data collected during ten observations made with the Proportional Counter Array (PCA) on board RXTE during eight consecutive days following the decay from the peak. The BATSE data of the outburst are also presented. In order to understand the nature of the system and estimate its distance, we make use of near-infrared spectra and optical photometry obtained shortly after the peak of the outburst.

2. OBSERVATIONS

2.1. RXTE/PCA

RXTE observed the source 10 times over roughly 8 days. In order to follow the spectral/timing evolution, we extracted PCA spectra for each of the observation intervals in Table 1. For a description of the instrument see Jahoda et al. (1996). The intervals were chosen so that the flux decay during each interval was small in order to minimize the effect of spectral/timing variations. During the observation of April 3rd, the pointing direction was adjusted following a better positional determination for the X-ray source. The fluxes before the correction have been rescaled to take into account the slight mispointing.

The combined PCA and ASM light curve is plotted in Fig. 1. After a rapid rise to the peak in less than half a day (Smith et al. 1998), the flux decayed roughly exponentially with an e-folding time $\tau \sim 0.5$ days for two days. This value is consistent with the value of 0.56 d observed with BATSE (Harmon, Fishman & Paciesas 1998), although the energy range is different. Afterwards, the decay slowed down, until after MJD 50908 it was $\tau = 2.34 \pm 0.05$ days. Notice that the intermediate decay time scales reported with BeppoSAX (0.7-1.3 days, energy dependent, Frontera et al. 1998) and with ASCA (1.27 d, Ueda et al. 1998) come from the interval when the flattening takes place (see Fig. 1), while the higher value obtained from the second BeppoSAX pointing is consistent with our estimate. The values reported by Revnivtsev, Emelyanov & Borozdin (1998) from the same PCA data are consistent with our determination.

We searched the 1.2-3.5 keV flux using the propane layer counts of the PCA (April 1–3) and found no deviations from a smooth decay comparable to those seen by SAX and ASCA in the sub-keV light curve.

2.2. BATSE hard X-ray observations

XTE J0421+056 was detected by the Burst and Transient Source Experiment (BATSE) on board the Compton Gamma Ray Observatory (CGRO). The BATSE Earth Occultation Technique was used to derive the flux and spectra of the source in the energy range 20 keV–1 MeV. This technique allows the flux of a bright hard X-ray or gamma ray source to be sampled at times when the source rises above or sets below the Earth’s limb. For more details, see Fishman et al. (1989).

In the 20–100 keV energy range covered by BATSE the light curve shows a very rapid rise (~ 0.1 day), peaking at March 31.98 \pm 0.075, followed by a rapid decline with an e-folding time which matches that observed early-on with the PCA (~ 0.56 day).

On the decline (MJD 50904 to 50905.0) the BATSE spectrum is well modeled by a power law with photon number index of -3.9 ± 0.3 . In comparison to other BHC transients this is a fairly soft spectrum. The BATSE data are compatible with our fits to the 2–25 keV data (see Section 3.1). There is marginal evidence for the hard X-ray spectrum being harder during the rise and/or peak.

2.3. Infrared

Infrared spectroscopic observations of CI Cam were carried out across the J-, H- and K-bands shortly after the peak of the outburst, on 1998 May 5 (J and K) and May 6 (H), at the UK Infrared Telescope (UKIRT). The CGS4 instrument was used with a 0.6 arcsec slit width and a spectral resolution of around $0.003 \mu\text{m}$. A discussion of these extremely rich emission line spectra, amongst the most detailed ever obtained for an X-ray binary, can be found in Clark et al. (1998a), in which 88 of more than 122 emission lines present in the spectrum are identified.

3. RESULTS

3.1. X-ray spectra

The selection of data for our energy spectral analysis was done in a standard way. Only data well above the Earth’s limb ($>10^\circ$), with all 5 PCU’s on, stable pointing, and full housekeeping were selected.

The background spectra were estimated with the FTOOLS *pcabackest* (V2.01) with the standard VLE+activation model for early (April 1st to 5th) observations. In the later observations the ”faint” (L7/240) model was used for the background estimation. The deadtime correction factor was calculated for each background and source PHA spectrum. The source PHA spectra were normalized by assuming that there were no detectable source counts above 60 keV. This was done to reduce the effects of systematic errors in the estimated background. Our fits were restricted to the 2–25 keV range where the response of the PCA is best determined. To account for unknown systematic error a 1% increase in the formal errors was applied to each PHA spectrum.

All fits included a component to take into account interstellar and intrinsic absorption from a cold absorber. An emission line near 6.5 keV is obvious in the raw PHA spectra of the early observations. Such a line was included in all fits. Various simple models were used to model the continuum. Of these a simple power law or blackbody type models did not fit the data, producing unacceptably high χ^2 values. A bremsstrahlung, broken power-law, a cutoff power-law or a power-law with a high energy cutoff produced much better (though not formally acceptable) fits. The quality of these fits were similar. We obtained results very similar to those of Revnivtsev et al. (1998) using the absorbed cutoff power-law and line model. In all cases except observations H and I better (90% confidence using the F-test) fits were obtained using a absorbed power-law with high-energy cutoff and line model. The high-energy cutoff *HC* is a multiplicative modification of a power law of the form $HC = \exp((E_{cut} - E)/E_{fold})$ for $E > E_{cut}$ and $HC = 1$ for $E < E_{cut}$.

The fit results of this model are presented in Table 2. The timing history of parameters showing significant variability is plotted in Fig. 2. No matter which continuum model was used, the overall trends remain unchanged. It is evident that the spectrum softens with time; the power law steepens and the folding energy moves from 11 keV at peak down to near 6 keV for the last

observation. Interestingly, the absorption increases from an initial (at peak luminosity) value near $2.2 \times 10^{22} \text{cm}^{-2}$ to near $3.8 \times 10^{22} \text{cm}^{-2}$, then decreases rapidly to become unmeasurable with the PCA. The actual values depend upon the model used. The initial increase in N_H is more dramatic when a cutoff power-law model is used for the continuum model. Our N_H measurements are not consistent with those from the contemporaneous SAX TOO1 observation, ours being considerably lower (see Orr et al. 1998). Notice that the ASCA observation is also contemporaneous with the SAX TOO1 and our I/J/K observations, and the value reported for N_H is marginally consistent with our upper limits (Ueda et al. 1998). The values for SAX TOO2 are consistent with our upper limits (Orr et al. 1998). All we can conclude is that the value of N_H is strongly model-dependent, although it would be difficult to interpret in this fashion the strong changes in absorption that we see between our early observations (A–G) and the later ones (H–R). The line flux decreases as the overall luminosity and power-law flux decreases. Initially the line flux is 4.8% of the power-law flux, with a slight increase to 5.5% in observations E,F and G followed by a slow decrease to 2.7% in the last observation.

The line energies are all near 6.5 keV in contrast to the near 6.7 keV measured using ASCA and SAX. This discrepancy is too large to be due to uncertainties in the energy calibration of the PCA, but could be due to an interaction between the Xenon edges of the response matrix and the continuum/line model (Jahoda, priv. comm.). We did find that the energy of the iron line was model dependent. In fact a simple power-law model yielded a line energy near 6.7 keV. The two SAX observations show no difference in the line energy (Orr et al. 1998), in contrast to the shift claimed by Revnivtsev et al. (1998) and evident in our fits with a cutoff power law model and to a lesser extent with the power-law with high energy cutoff model. Since the continuum shape is changing markedly, we consider it likely that the line shift is caused by the same coupling between response matrix and the model used to explain the lower energy of the iron line. With the more complicated model of a cutoff power-law and edge we find no evidence for a change in line energy.

With the above simple models, the residuals generally show a peak/dip structure in the 8–10 keV range (Fig. 3). In some observations (i.e. H,I with the high energy cutoff model) the residuals in the 15–25 keV range dominate the final χ^2 values. This indicates the need for an extra component in the model of the PHA spectra. We found that the blackbody component of the "standard" BHC model (disk-blackbody and cutoff power-law) did not improve the fits and so was unnecessary. Adding an either an extra line near 8 keV, an edge or smeared edge near 9.12 keV (the energy expected for a iron fluorescence line near 6.7 keV; Nagase 1989), or an extra power law (specifically using a broken power-law instead of a power-law with the high energy cutoff model) produced significantly better (95% confidence) fits for the earlier (before H) observations.

The line energy of the extra line is near 8.3 keV and we find no evidence for a change in line energy. The line flux also decreases approximately in step with the power law component flux; fractionally about 0.39% (lower in obs H,I,J at 0.28%). The edge or smeared edge component always has a small depth (MaxTau \approx 0.1) and a fairly narrow width (\approx 1 keV). For the later observations an extra component was not warranted both by either the improvement in χ^2 or the

resulting best fit parameters i.e. the 8 keV line or edge became negligible, or the two power law slopes became the same. An example of the fit residuals for various models is shown in Fig. 3 for observation B (high flux, high absorption).

These four models are all equally good representations of the data. Thus we conclude that the spectra of CI Cam is more complex than the canonical X-ray transient, with no substantive evidence in the PCA data for moving lines indicative of relativistic jets.

3.2. X-ray variability

To study the X-ray variability characteristics of XTE J0421+560 we made power density spectra for each of the individual data stretches listed in Table 1. Timing analyses show that the broad-band (1–4096 Hz) X-ray power density spectra were flat throughout the outburst and probably consistent (given the model uncertainties) with detector-modified Poisson noise (Zhang et al. 1996, Morgan, Remillard & Greiner 1997). Thus the only excess X-ray variability exhibited by CI Cam during its outburst decay was a smooth fading of the source flux (which provides significant power at frequencies $\ll 1$ Hz).

Upper limits (95%-confidence) on the total 1–4096 Hz excess variability are 0.5% rms (dominated by systematic uncertainties) during the early (high count-rate) observations, increasing to $\sim 10\%$ rms towards the end of the outburst, with no detection registered at any time. No coherent or quasiperiodic features were seen in the power spectra. Upper limits on coherent pulsations (95% confidence, 0.01–4096 Hz, 2–60 keV) are 0.1% rms for the early observations, increasing to 2% by the end. In the restricted 5–12 keV band, limits increase from 0.1% to 5%. Upper limits on QPO features are width-dependent; increasing from 0.2%, 0.4%, and 0.7% rms to 6%, 10%, and 15% rms over the course of the outburst decay for features 1/8, 1 and 8 Hz wide, respectively.

4. The infrared/optical spectrum of CI Cam

Comparing the quiescent optical/near-IR magnitudes listed in Bergner et al. (1995) to the outburst values indicates that CI Cam had clearly brightened during the outburst. In order to determine the nature of the bright mass donor and the spectrum of the outburst component in the infrared, we first fit the quiescent optical – near-IR data. These data were fit by means of a combined Kurucz plus optically thin dust (Waters, Coté & Geballe 1988) model. This fit to the optical/IR spectral energy distribution is illustrated in Fig. 4; uncertainties in $E(B-V)$ and R_V (the ratio of total to selective extinction) are indicated on the figure. The data are consistent with a hot ($T_{\text{eff}} \geq 22000\text{K}$; i.e. B2 or earlier) star plus a large mass ($\geq 0.002M_{\odot}$) of heated dust. Also indicated in Fig. 4 are the IRAS 12, 25 & 60 μm fluxes, as well as the 100 μm upper limit; these fit the dust model very well. The value of R_V (3.7, compared to the normal interstellar value of 3.1)

indicates on average larger particles in the dust shell, consistent with strong radiation pressure having removed the smaller ($\leq 0.3\mu\text{m}$; Steenman & Thé 1991) particles.

The quiescent infrared data as well as the fact that both components in the optical/IR spectrum brighten during outburst clearly indicate that CI Cam is not a symbiotic system containing a red giant, but that it contains a hot massive star surrounded by a substantial dust shell. We conclude that these data are more consistent with a B[e] classification (Hubert & Jaschek 1997 and references therein) for the system. An LBV (Luminous Blue Variable, see Humpreys & Davidson 1994) interpretation is plausible, but if this is the case it is has to be much more distant than 2 kpc, in contradiction with the upper limit on the distance obtained by Clark et al. (1998b). We note that Lamers et al. (1997) list the system as being ‘unclassified / compact planetary nebula ?’. However, the IRAS 25/12 μm flux ratio of CI Cam (0.35) places it firmly outside the IRAS color-color box occupied by planetary nebulae ($F_{25}/F_{12} > 4.0$, see e.g. Miroschnichenko 1997), excluding this possibility. Clark et al. (1998a) discuss the highly stratified and/or asymmetric circumstellar environment of CI Cam, indicated by emission from both high excitation HeII and low excitation NaI and CO-band emission; this again is consistent with a B[e] model for the system.

In Fig. 4 we indicate VRI outburst photometry (from Clark et al. 1998b) and our IR spectra, dereddened according to the anomalous extinction law fitted to the quiescent data. After subtraction of the quiescent spectra (dominated by the dust emission for $\lambda \geq 1\mu\text{m}$) we find that the outburst excess across the JHK near-IR bands is still very red. The cause of this red outburst component is not clear; it may indicate heating of the dust during the outburst, enhanced dust formation since the quiescent data of Bergner et al. (1995), or a more exotic mechanism such as high-frequency synchrotron emission. The optical – infrared colors are probably not compatible with additional quantities of new dust (which would include small grains and hence a different value of R_V from quiescence), and a synchrotron origin would have implied flux densities in the radio regime which were far higher than those observed, so we favor an explanation of significant, rapid heating of the existing dust shell during the outburst to explain the red color of the outburst component in the near-infrared.

Our model fits constrain the distance to CI Cam to be ≥ 350 pc. The total A_V from our fit is 4.4 ± 0.2 mag. In the direction of CI Cam, the local Orion spiral arm lies at a distance of 200 – 400 pc; the more distant Perseus spiral arm at around 2-4 kpc (Gilmore, King & van der Kruit 1989). It seems quite plausible that CI Cam lies in the Perseus spiral arm. At a distance of 2 kpc, its (quiescent) luminosity is around $10^5 L_\odot$, while during outburst (assuming the same spectral distribution) it is 4 times higher.

Zorec (1997) has independently estimated the temperature, luminosity, distance and reddening to CI Cam from the optical observations of Bergner (1995). All the values derived (from optical quiescent observations) are consistent with those arrived at in our independent analysis, and we adopt his best distance estimate of 1750 pc to the system. At this distance the mass donor is

on or near the main sequence with a mass of around $20M_{\odot}$. As evidenced by the presence of high-excitation lines in the optical and near-infrared spectrum, during outburst the enhanced emission in the optical was dominated by hot gas. The brightening in the infrared during outburst is due to reprocessing of the enhanced optical emission by the circumstellar dust.

5. Discussion

At the distance of ~ 2 kpc the peak X-ray luminosity of XTE J0421+560 (several 10^{37} erg s^{-1}) is high enough that we can exclude accretion onto a white dwarf as the cause of the X-ray emission. Since the X-ray spectrum of XTE J0421+560 is not extremely soft, we can also exclude thermonuclear burning on a white-dwarf surface as the source of the X-ray emission (this would produce a supersoft X-ray source, see Kahabka & Van den Heuvel 1997). The soft component detected by BeppoSAX and ASCA has a spectrum similar to that of supersoft X-ray sources (see Ueda et al. 1998), but its relatively high temperature (0.12 keV) and relatively fast variability have not been observed among those sources. We can also exclude a nova explosion: the X-ray luminosity would not be inconsistent, but the X-ray spectrum is harder than in novae and the optical spectrum does not have the features of a nova in outburst.

During the outburst the optical luminosity of CI Cam increased by an order of magnitude, on a time scale of order a day. It is plausible that this increase is caused by reprocessing of X rays. Such reprocessing dominates the optical emission of low-mass X-ray binaries (Van Paradijs & McClintock 1995), but in CI Cam the ratio of optical to X-ray luminosity outburst is much higher than in these objects, by about a factor of 10^3 . This indicates that the geometry of the reprocessing material in CI Cam is different from that in LMXB (in the latter it is an accretion disk).

To the best of our knowledge, the only object that shows properties similar to CI Cam, is the LMC transient A 0538–66 (see Corbet et al. 1997 and references therein). The source was discovered with Ariel V by White & Carpenter (1978), who observed two outbursts, each lasting several hours only, during which a peak luminosity close to 10^{39} erg s^{-1} was reached. Additional brief (less than 12 hours) X-ray outbursts were detected by Johnston et al. (1980). Low-amplitude ($<10^{37}$ erg/s) X-ray outbursts have also been detected by Corbet et al. (1997) with ASCA and Mavromatakis & Haberl (1993) with ROSAT. The X-ray outbursts, which recur at the orbital period of 16.7 days (Johnston et al. 1980) and have durations between a few hours and ~ 10 days, are accompanied by optical outbursts, in which the brightness increases from a quiescent value $V = 14.7$ by up to 2.5 mag (see, e.g., Densham et al. 1983). The quiescent optical flux is dominated by the photospheric emission of the B2 IIIe companion star. The optical outbursts last for several days (Densham et al. 1983). These outbursts recur during relatively short intervals (a few months) of activity, alternated by long (many years) periods of quiescence. Ponman, Skinner & Bedford (1984) found a strong anti-correlation between X-ray intensity and the column density N_{H} for A 0538–66. Mavromatakis & Haberl (1993) report two outburst of different duration from

the ROSAT all-sky survey, both with mean luminosity of a few 10^{37} erg/s. Combining the ROSAT PSPC data with older Einstein MPC data, they quantify the soft excess reported by Ponman, Skinner & Bedford (1984): they fit the spectrum with a cut-off power law with photon index 1.2 and cutoff energy ~ 11 keV, plus a soft component which can be described by a blackbody with a temperature of 0.25 keV.

Thus, with respect to the brevity of the X-ray outbursts, the large ratio of optical to X-ray luminosity, the X-ray spectrum and the irregular occurrence of activity periods CI Cam is very similar to A 0538–66. It differs with respect to the relation between N_{H} and X-ray flux, to the frequency of the outbursts, and to the physical properties of the circumstellar envelope of the companion, as reflected in their spectral classifications (B[e] for CI Cam, Be for A 0538–66).

A 0538–66 is a member of the class of Be/X-ray transients, in which recurrent outbursts of X rays occur near periastron passage of the compact star in its eccentric orbit around the Be companion star. The compact star then enters the dense inner region of the slow equatorial wind of the Be star, part of which is captured and accreted at a rate that depends on the local density in the wind and the relative velocity of the neutron star through this wind. The shedding of mass by the Be star in its equatorial wind occurs at a strongly variable rate, which leads to finite trains of X-ray outbursts, separated by the orbital period (see, e.g., Bildsten et al. 1997). The compact object in A 0538–66 is a neutron star, as shown by the 69 ms pulsations in its X-ray intensity (Skinner et al. 1982). Apparently the solid angle of the Be star envelope intercepting X rays is large enough that a substantial fraction of the X-ray luminosity is reprocessed into low-energy photons, producing the soft component and the optical outburst.

The fact that for CI Cam the optical luminosity during outburst exceeds the X-ray luminosity (by a factor >10) can be understood as a result of shielding: we do not see the primary X-ray emission but only a fraction which has been scattered by the material surrounding the compact object. This idea also provides a natural explanation for the lack of variability at frequencies above 1 Hz: scattering-induced travel time delays of the observed photons have smeared out variability at these frequencies. The effect of such smearing has also been observed in Cyg X-3 (Berger & Van der Klis 1994).

In the case of A 0538–66 the optical luminosity during outbursts is a substantial fraction (but less than unity) of the X-ray luminosity. Also, pulsations are detected. This indicates that in this source we see the primary X-ray emission in a relatively unobstructed fashion. The different spatial arrangement of the material surrounding the compact object in CI Cam relative to the line of sight to the observer (which may simply be a matter of different inclination angle) provides a possible explanation for the different relations between N_{H} and the X-ray flux seen in CI Cam and A 0538–66 (see Ponman, Skinner & Bedford 1984).

In summary, although the nature of the compact star in CI Cam has not been revealed by the observations presented here, the properties of CI Cam as seen during its 1998 outburst suggest it is a B[e]/X-ray binary. In all Be/X-ray binaries for which we have definite information about

the nature of the compact star, this is a neutron star (i.e. pulsator). However, CI Cam has been detected as a relatively bright radio source (Hjellming & Mioduszewski 1998a). The detection of radio emission at all would seem to exclude a high magnetic field neutron star (X-ray pulsar) from the observed strong anticorrelation between the two properties (Fender et al. 1997). The strength of the radio emission at the peak of the outburst (~ 1 Jy at cm wavelengths) is more typical of black hole candidates such as GRO J1655-40 than of low magnetic field neutron star transients such as Aql X-1 (typically around a few mJy), although several strong radio sources e.g. SS 433, Cyg X-3, LSI+61 303 may contain neutron stars (see Hjellming & Han 1995, Fender, Bell Burnell & Waltman 1997). In conclusion, our results suggest that XTE J0421+560/CI Cam is a peculiar system consisting of a B[e] star and either a low magnetic field neutron star or a black hole. In either case it would be the first system of its kind.

MvdA acknowledges financial support from NWO/NFRA grant 781-76-015. RPF thanks Simon Clark for useful discussions and Tom Geballe for obtaining and reducing the IR spectra, and was supported by EC Marie Curie Fellowship ERBFMBICT 972436. SD and JVP acknowledge the support of LTSA grant number NAG 5-6021.

REFERENCES

- Berger, M., van der Klis, M., 1994, *A&A*, 292, 175
- Bergner, Yu K., Miroshnichenko, A.S., Yudin, R.V., Kuratov, K.S., Mukanov, D.B., Shejkina, T.A., 1995, *A&A Suppl. Ser.*, 112, 221
- Bildsten, L., et al., 1997, *ApJ Suppl.*, 113, 367
- Clark, J.S., Steele, I.A., Fender, R.P., Coe, M.J., 1998a, *MNRAS*, submitted.
- Clark, J.S., et al., 1998b, *MNRAS*, submitted.
- Corbet, R.H., Charles, P.A., Southwell, K.A., Smale, A.P., 1997, *ApJ*, 476, 833
- Densham, R.H., Charles, P.A., Menzies, J.W., van der Klis, M., van Paradijs, J., 1983, *MNRAS*, 205, 1117
- Fender R.P., Bell Burnell S.J., Waltman E.B., 1997, *Vistas Astron.*, 41, 3
- Fender, R.P., Roche, P., Pooley, G.G., Chakrabarty, D., Tzioumis, A.K., Hendry, M.A., Spencer, R.E., 1997 *Proceedings 2nd INTEGRAL Workshop ‘The Transparent Universe’*, St. Malo, France, 16-20 September 1996, *ESA SP-382*, p303
- Fishman, G.J., et al., 1989, in *Proc. of the Gamma Ray Observatory Science Workshop*, ed. Johnson W.N., Sec. 3, p.47
- Frontera, F., et al., 1998, *A&A*, 339, L69
- Garcia, M.R., Berlind, P., Barton, E., McClintock, J.E., McCarthy, J., 1998, *IAU Circ.*, No. 6865
- Gilmore, G., King, I., van der Kruit, P., 1989, “The Milky Way as a Galaxy”, 19th Saas-Fee advanced course of the Swiss Society of Astrophysics and Astronomy, Geneva.
- Harmon, B.A., Fishman, G.J., & Paciesas, W.S., 1998, *IAU Circ.*, No. 6874
- Hjellming R.M., Han X., 1995, in ‘X-ray binaries’, eds. Lewin W., Van Paradijs, J., Van den Heuvel E.P.J., Cambridge University Press, Cambridge, 308
- Hjellming, R.M., Mioduszewski, A.J., 1998a, *IAU Circ.*, No. 6857
- Hjellming, R.M., Mioduszewski, A.J., 1998b, *IAU Circ.*, No. 6872
- Hubert A.M., Jaschek C., 1997, Eds, ‘B[e] stars’, *Ap. & SS library vol. 233*, Kluwer
- Humphreys, R.A., Davidson, K. 1994, *PASP* 106, 1025
- Hynes, R.I., Roche, P., Haswell, C.A., et al., 1998, *IAU Circ.*, No. 6871

- Jahoda, K., et al., 1996, in Proc. SPIE 2808, EUV, X-ray and Gamma-Ray Instrumentation for Astronomy VII, ed. D.H.W. Siegmund & M.A. Gummin (Bellingham: SPIE), 59
- Johnston, M.D., Griffiths, R.E., Ward, M.J., 1980, *Nature*, 285, 26
- Kahabka, P., Van den Heuvel, E.P.J., 1997, *ARA&A*, 35, 69
- Lamers J.G.L.M., Zickgraf F.-J., De Winter D., Houziaux L., Zorec J., In ‘B[e] stars’, Hubert A.M., Jaschek C., 1997, Eds, Ap. & SS library vol. 233, Kluwer, p. 277
- Levine, A.M., Bradt, H., Cui, W., Jernigan, J.G., Morgan, E.H., Remillard, R., Shirey, R.E., Smith, D.A., 1996, *ApJ* 469, L33
- Mavromatakis, F., Haberl, F., 1993, *A&A*, 274, 304
- Miroshnichenko, A.S., 1997, in “B[e] stars”, eds. A.M. Hubert & C. Jaschek, Kluwer Academic Publishers, Dordrecht.
- Morgan, E.H., Remillard, R.A., Greiner, J., 1997, *ApJ* 482, 993
- Nagase, F., 1989, *PASJ*, 41, 1
- Orlandini, M., Dal Fiume, D., Frontera, F., Piro, L., Parmar, A.N., 1998, *IAU Circ.*, No. 6868
- Orr, A., Parmar, A.N., Orlandini, M., Frontera, F., Dal Fiume, D., Segreto, A., Santangelo, A., Tavani, M., 1998, *A&A*, 340, L19
- Paciesas, W.S., Fishman, G.J., 1998, *IAU Circ.*, No. 6856
- Ponman, T.J., Skinner, G.K., Bedford, D.K., 1984, *MNRAS*, 207, 621
- Van Paradijs, J., McClintock, J.E., 1995, in ‘X-ray binaries’, eds. Lewin W., Van Paradijs, J., Van den Heuvel E.P.J., Cambridge University Press, Cambridge, p.58
- Revnivtsev, M., Emelyanov, A., Borozdin, K., 1998, *Astronomy Letters*, in press.
- Robinson, E.L., Welsh, W.F., Adams, M.T., Cornell, M.E., 1998, *IAU Circ.*, No. 6862
- Skinner, G.K., Bedford, D.K., Elsner, R.F., Leahy, D., Weisskopf, M.C., Grindlay, J., 1982, *Nature*, 297, 568
- Smith, D., Remillard, R., Swank, J., Takeshima, T., Smith, E., 1998, *IAU Circ.*, No. 6855
- Steenman, H., Thé, P.S., 1991, *Ap&SS*, 184, 9
- Ueda, Y., Ishida, M., Inoue, H., Dotani, T., Greiner, J., Lewin, W.H.G., 1998, *ApJ*, 508, L167
- Wagner, R.M., Starrfield, S.G., 1998, *IAU Circ.*, No. 6857

Waters, L.B.F.M., Côté, J., Geballe, T.R., 1988, A&A, 203, 348

White, N.E., Carpenter, G.F., 1978, MNRAS, 183, 11p

Zhang, W., Morgan, E.H., Jahoda, K., Swank, J.H., Strohmayer, T.E., Jernigan, G., Klein, R.I., 1996, ApJ 469, L29

Zorec J., 1997, In ‘B[e] stars’, Hubert A.M., Jaschek C., 1997, Eds, Ap. & SS library vol. 233, Kluwer, p. 27

Table 1. Observation log. Times are in UT, exposures in seconds. the MJD values refer to the start of the observation.

ID	Date	Start	End	Exp.	MJD
A	1998 Apr 1	1:55	2:14	1028	50904.0798
B	1998 Apr 1	2:14	2:32	1014	50904.0930
C	1998 Apr 1	3:38	3:50	667	50904.1514
D	1998 Apr 1	6:41	7:10	1597	50904.2784
E	1998 Apr 1	8:20	9:14	2484	50904.3472
F	1998 Apr 1	9:56	10:10	769	50904.4139
G	1998 Apr 1	10:29	10:50	1199	50904.4368
H	1998 Apr 2	6:40	10:47	8023	50905.2777
I	1998 Apr 3	5:05	5:51	2063	50906.2118
J	1998 Apr 3	5:53	9:09	5219	50906.2451
K	1998 Apr 3	11:37	11:49	701	50906.4840
L	1998 Apr 4	6:40	9:14	3144	50907.2777
M	1998 Apr 5	6:39	10:08	7805	50908.2770
N	1998 Apr 6	3:27	4:28	1502	50909.1437
O	1998 Apr 7	2:36	4:26	4180	50910.1083
P	1998 Apr 7	18:08	18:22	743	50910.7555
Q	1998 Apr 8	3:45	6:02	5888	50911.1562
R	1998 Apr 9	6:38	7:30	3084	50912.2764

Table 2. Spectral parameters for the fits to the RXTE/PCA data described in the text (power-law+gaussian line, modified by a high-energy cutoff). Errors are 1σ . Reduced χ^2 are for 47 degrees of freedom. Observation P was too short to obtain meaningful values.

ID	Rate cts/s	N_H cm^{-2}	Γ	E_l keV	W_l keV	EQW_l eV	E_{cut} keV	E_{fold} keV	F_{pl} erg/cm ² /s	F_l erg/cm ² /s	χ^2
A	32314	2.20±0.36	1.42± 0.09	6.57±0.03	0.49±0.03	642	5.20±0.46	11.23± 0.75	9.63×10 ⁻⁸	4.66×10 ⁻⁰⁹	0.84
B	31596	2.43±0.36	1.49± 0.09	6.54±0.03	0.47±0.06	608	4.47±0.46	11.68± 0.75	9.55×10 ⁻⁸	4.23×10 ⁻⁰⁹	0.88
C	27217	2.76±0.38	1.54± 0.10	6.55±0.03	0.34±0.18	637	5.44±0.48	11.51± 0.79	8.26×10 ⁻⁸	3.98×10 ⁻⁰⁹	0.94
D	23297	3.51±0.36	1.57± 0.08	6.53±0.03	0.30±0.04	645	5.56±0.45	12.27± 0.81	7.29×10 ⁻⁸	3.53×10 ⁻⁰⁹	0.98
E	19898	3.76±0.36	1.53± 0.08	6.53±0.03	0.48±0.06	697	5.37±0.42	11.38± 0.72	6.21×10 ⁻⁸	3.29×10 ⁻⁰⁹	1.10
F	17325	3.70±0.39	1.51± 0.09	6.52±0.03	0.25±0.03	719	5.47±0.42	10.96± 0.74	5.36×10 ⁻⁸	2.95×10 ⁻⁰⁹	1.33
G	16386	3.69±0.37	1.48± 0.09	6.53±0.03	0.24±0.03	721	5.46±0.39	10.90± 0.65	5.07×10 ⁻⁸	2.81×10 ⁻⁰⁹	1.18
H	3225	< 0.082	1.54± 0.04	6.55±0.03	0.32±0.03	675	5.83±0.22	10.09± 0.22	8.63×10 ⁻⁹	4.62×10 ⁻¹⁰	0.95
I	947	< 0.23	2.12 ^{+0.06} _{-0.03}	6.53±0.03	0.29±0.06	636	6.83 ^{+0.40} _{-0.31}	12.39 ^{+0.83} _{-0.49}	2.58×10 ⁻⁹	1.22×10 ⁻¹⁰	1.42
J	810	< 0.15	2.11 ^{+0.04} _{-0.03}	6.58±0.03	0.27±0.06	622	6.44 ^{+0.39} _{-0.27}	12.16 ^{+0.52} _{-0.39}	2.20×10 ⁻⁹	1.01×10 ⁻¹⁰	1.47
K	553	< 0.59	2.25 ^{+0.15} _{-0.29}	6.55±0.04	0.29±0.08	651	7.02 ^{+1.02} _{-0.40}	13.15 ^{+2.71} _{-0.71}	1.52×10 ⁻⁹	7.00×10 ⁻¹¹	0.86
L	288	< 0.57	2.46 ^{+0.29} _{-0.15}	6.58±0.05	0.33±0.06	673	6.65 ^{+0.40} _{-0.86}	12.27 ^{+0.71} _{-0.66}	8.39×10 ⁻¹⁰	3.64×10 ⁻¹¹	0.97
M	138	< 0.24	2.69 ^{+0.07} _{-0.03}	6.56±0.03	0.27±0.07	649	7.18 ^{+0.34} _{-0.27}	9.78 ^{+0.80} _{-0.59}	3.92×10 ⁻¹⁰	1.60×10 ⁻¹¹	1.19
N	86	< 0.16	2.79± 0.05	6.57±0.04	<0.26	655	7.30±0.48	8.10 ^{+1.50} _{-1.15}	2.48×10 ⁻¹⁰	9.77×10 ⁻¹²	1.43
O	57	< 0.25	2.92 ^{+0.08} _{-0.05}	6.55±0.04	<0.32	661	7.50±0.41	6.84 ^{+1.19} _{-0.93}	1.68×10 ⁻¹⁰	6.43×10 ⁻¹²	0.66
Q	41	< 0.24	2.98 ^{+0.07} _{-0.04}	6.63±0.07	<0.35	522	6.96 ^{+0.45} _{-0.65}	6.96 ^{+1.82} _{-1.22}	1.25×10 ⁻¹⁰	3.58×10 ⁻¹²	0.98
R	30	< 1.09	3.10 ^{+0.26} _{-0.09}	6.56±0.09	<0.29	490	7.33 ^{+0.63} _{-0.85}	6.25 ^{+2.59} _{-1.55}	9.39×10 ⁻¹¹	2.51×10 ⁻¹²	0.51

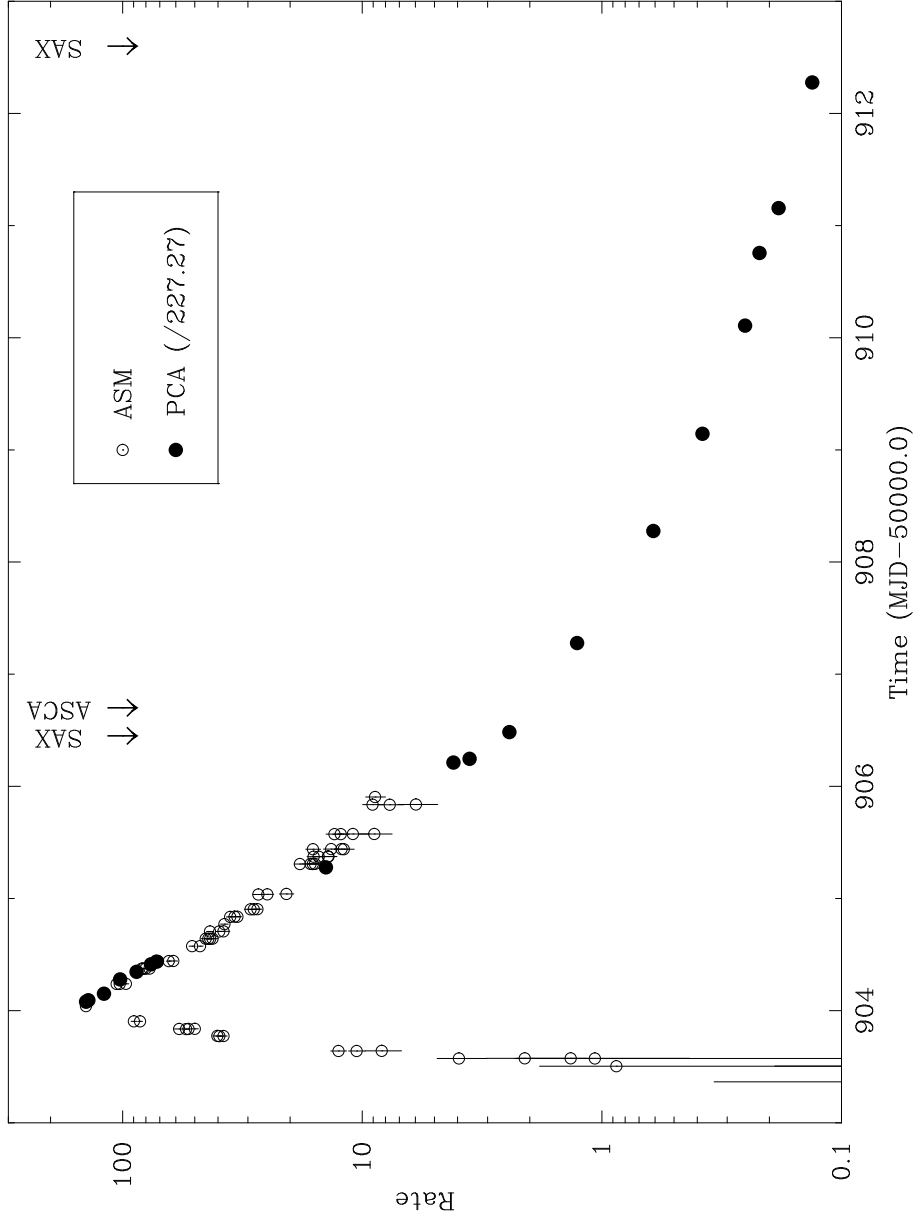


Fig. 1.— Combined ASM/PCA light curve of XTE J0421+560. The ASM points are from http://space.mit.edu/XTE/ASM_lc.html, the PCA points are from this work. The PCA rate has been renormalized to match the ASM rate at the peak. The arrows indicate the middle of the ASCA and BeppoSAX observations.

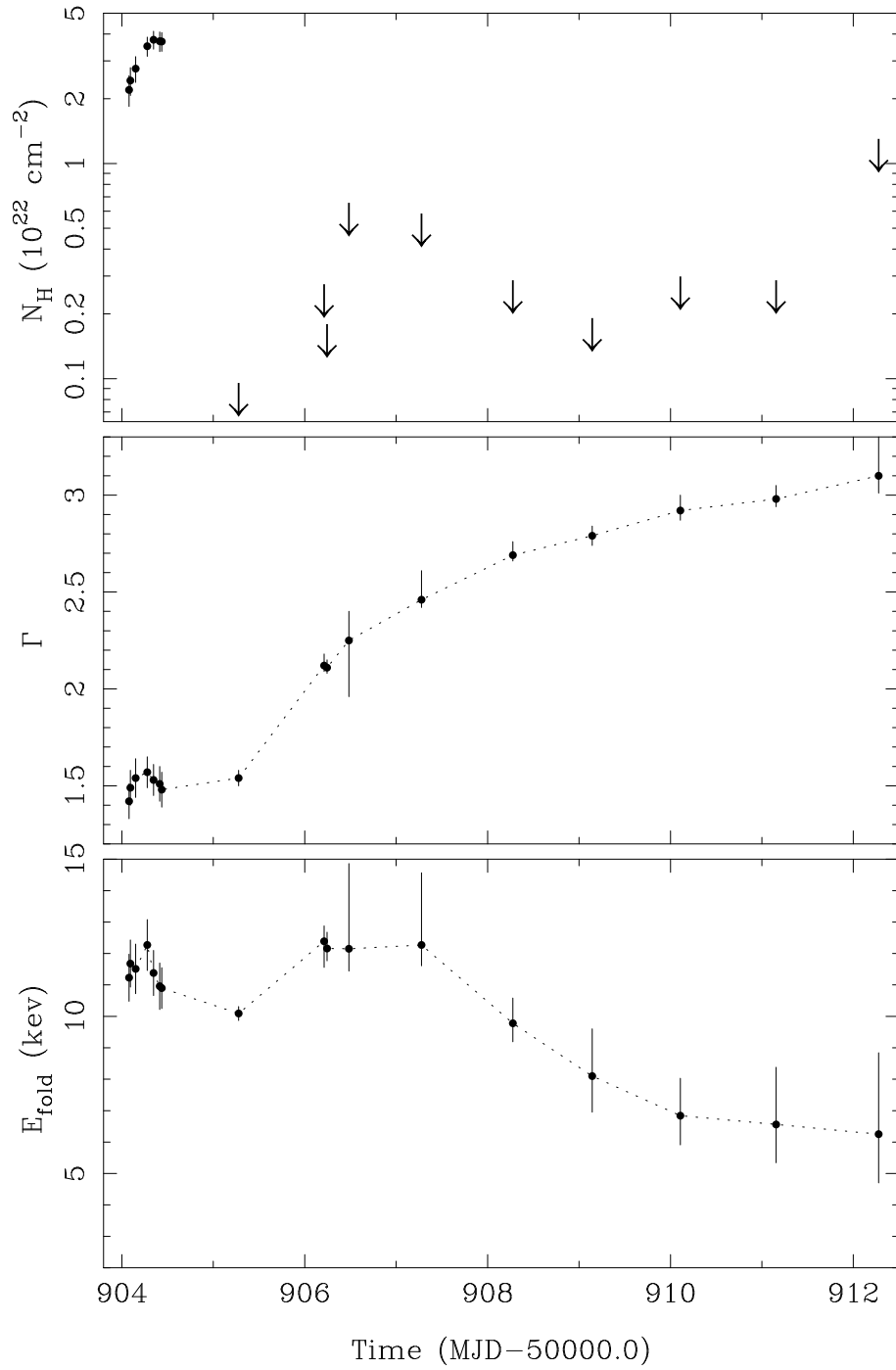


Fig. 2.— Time history of variable parameters in the X-ray spectrum of XTE J0421+560. Top panel: absorption; middle panel: power law photon index; bottom panel: cutoff energy.

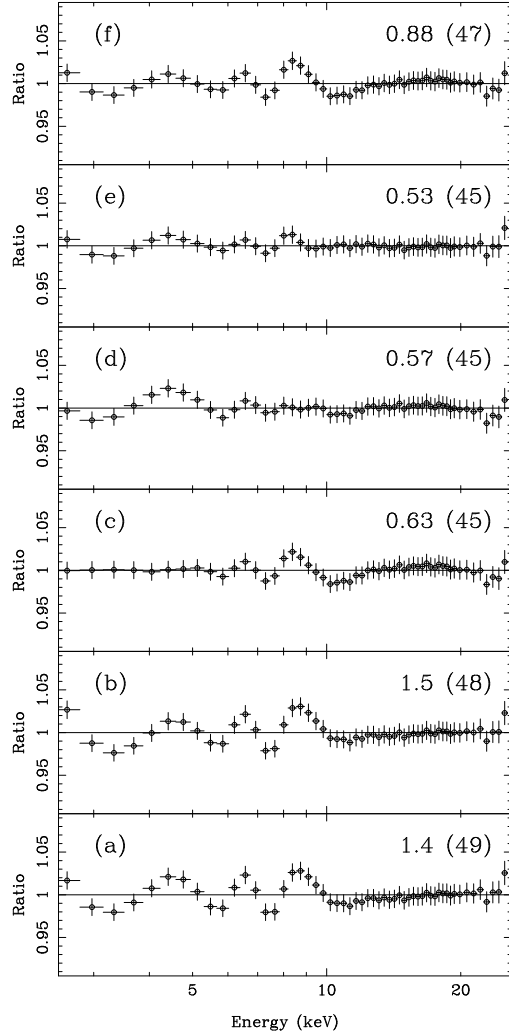


Fig. 3.— Ratio data/model for the spectrum of observation B for different spectral models described in the text. The numbers in each panel are reduced χ^2 and number of degrees of freedom. The models are: (a) bremsstrahlung plus gaussian line; (b) cutoff power law plus gaussian line; (c) broken power plus gaussian line; (d) power law with high energy cutoff plus two gaussian lines; (e) power law with high energy cutoff plus gaussian line and absorption edge; (f) power law with high energy cutoff plus gaussian line.

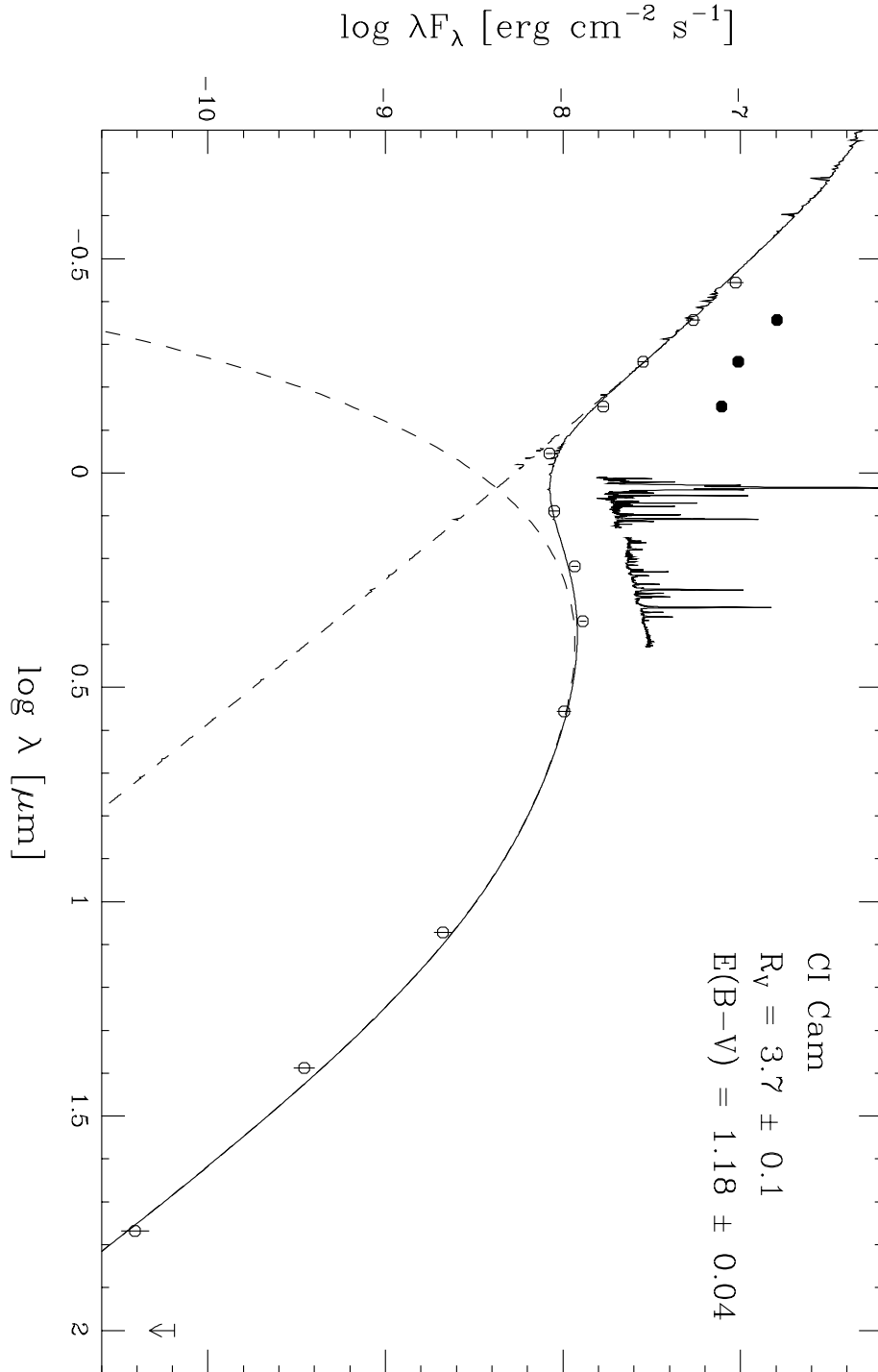


Fig. 4.— Fit to the observed quiescent optical and near-IR photometry (open symbols) of CI Cam with a Kurucz hot star + optically thin dust (dashed lines; combined model solid line) and anomalous reddening model. Also indicated are the IRAS 12, 25 and 60 μ m flux densities (plus the 100 μ m upper limit), which are consistent with the dust model. Also indicated are optical photometry and infrared spectra obtained during the outburst. Subtraction of the quiescent emission reveals the outburst component in the near-IR to be very red, indicative of rapid heating of the dust shell during the outburst.